Anal. Chem. **2004,** *76,* 3162−3170

Integrated Portable Genetic Analysis Microsystem for Pathogen/Infectious Disease Detection

E. T. Lagally,[†] J. R. Scherer,[‡] R. G. Blazej,[†] N. M. Toriello,[†] B. A. Diep,[§] M. Ramchandani,[§,||] G. F. Sensabaugh,[§] L. W. Riley,[§] and R. A. Mathies*[,†,‡]

Chemistry Department, University of California, Berkeley, California 94720

An integrated portable genetic analysis microsystem including PCR amplification and capillary electrophoretic (CE) analysis coupled with a compact instrument for electrical control and laser-excited fluorescence detection has been developed. The microdevice contains microfabricated heaters, temperature sensors, and membrane valves to provide controlled sample positioning and immobilization in 200-nL PCR chambers. The instrument incorporates a solid-state laser and confocal fluorescence detection optics, electronics for sensing and powering the PCR reactor, and high-voltage power supplies for conducting CE separations. The fluorescein-labeled PCR products are amplified and electrophoretically analyzed in a gel-filled microchannel in <10 min. We demonstrate the utility of this instrument by performing pathogen detection and genotyping directly from whole *Escherichia coli* and *Staphylococcus aureus* cells. The *E. coli* detection assay consists of a triplex PCR amplification targeting genes that encode 16S ribosomal RNA, the *fliC* flagellar antigen, and the *sltI* shigatoxin. Serial dilution demonstrates a limit of detection of 2−3 bacterial cells. The *S. aureus* assay uses a *femA* marker to identify cells as *S. aureus* and a *mecA* marker to probe for methicillin resistance. This integrated portable genomic analysis microsystem demonstrates the feasibility of performing rapid high-quality detection of pathogens and their antimicrobial drug resistance.

Genetic assays, including whole genome sequencing, are helping to establish the origins of life, the molecular mechanisms of disease processes, and the genetic contributions to complex phenotypes. Moving from conventional capillary array electrophoresis technologies to chip-based analysis systems has the potential to increase the efficiency and speed of these assays. Recent work in the field has focused on integration of sample preparation steps with high-resolution analysis to eliminate problems encountered in higher volume and nonintegrated formats. Particularly in the areas of clinical diagnostics and pathogen detection, faster integrated assays with lower and more quantitative molecular limits of detection are desired. Most importantly, small, portable systems for field-capable analysis are critical for timely detection and prevention efforts. Work to create such integrated portable systems has proceeded along two separate tracks. Fabrication of high-resolution, high-throughput analysis systems with integrated sample preparation seeks to speed assay times while minimizing sample consumption and maintaining accurate identification and typing. Second, development of portable real-time PCR systems, seeks to reduce the size of the analysis hardware to create field-capable analysis instruments.

Work in the first area has progressed rapidly, based on the original development of high-resolution microfabricated capillary electrophoresis (CE) systems. For example, our group has demonstrated simultaneous high-speed separation and detection of 384 PCR amplicons and 96 SNP markers as well as high-throughput sequencing on microfabricated glass capillary array electrophoresis devices.[1−3] These approaches have relied upon conventional off-chip sample preparation. A variety of integrated systems capable of combining several conventional molecular biology processes at the microliter-to-nanoliter volume scale have also been developed.[4] One of the most critical steps is the specific amplification of genetic material by PCR. An integrated PCR-CE microdevice consisting of a silicon reaction chamber attached to a glass CE analysis chip was first developed by Woolley et al.[5] This device was capable of amplifying 10 μL of sample in 15 min from a template concentration of 10^6 copies/μL and performed CE analysis of the products in less than 2 min. Subsequent chip-based amplification has been conducted in a variety of materials[6−12]

* Corresponding author: (fax) (510) 642-3599; (e-mail) rich@zinc.cchem.berkeley.edu.

[†] Joint UCB/UCSF Bioengineering Graduate Group.

[‡] Department of Chemistry.

[§] Division of Infectious Diseases, School of Public Health.

[||] Current address: NIH/NIAID, 9000 Rockville Pike, Building 10, 11B05, Bethesda, MD 20892.

(1) Paegel, B. M.; Emrich, C. A.; Wedemayer, G. J.; Scherer, J. R.; Mathies, R. A. *Proc. Natl. Acad. Sci. U.S.A.* **2002**, *99*, 574−579.

(2) Emrich, C. A.; Tian, H.; Medintz, I. L.; Mathies, R. A. *Anal. Chem.* **2002**, *74*, 5076−5083.

(3) Medintz, I.; Wong, W. W.; Berti, L.; Shiow, L.; Tom, J.; Scherer, J.; Sensabaugh, G.; Mathies, R. A. *Genome Res.* **2001**, *11*, 413−421.

(4) Northrup, M. A., Jensen, K. F., Harrison, D. J., Eds. *Micro Total Analysis Systems 2003*, Transducers Research Foundation, Inc.: Cleveland Heights, OH, 2003.

(5) Woolley, A. T.; Hadley, D.; Landre, P.; deMello, A. J.; Mathies, R. A.; Northrup, M. A. *Anal. Chem.* **1996**, *68*, 4081−4086.

(6) Belgrader, P.; Smith, J. K.; Weedn, V. W.; Northrup, M. A. *J. Forensic Sci.* **1998**, *43*, 315−319.

(7) Daniel, J. H.; Iqbal, S.; Millington, R. B.; Moore, D. F.; Lowe, C. R.; Leslie, D. L.; Lee, M. A.; Pearce, M. J. *Sens. Actuators, A* **1998**, *71*, 81−88.

(8) Wilding, P.; Kricka, L. J.; Cheng, J.; Hvichia, G.; Shoffner, M. A.; Fortina, P. *Anal. Biochem.* **1998**, *257*, 95−100.

(9) Waters, L. C.; Jacobson, S. C.; Kroutchinina, N.; Khandurina, J.; Foote, R. S.; Ramsey, J. M. *Anal. Chem.* **1998**, *70*, 5172−5176.

(10) Waters, L. C.; Jacobson, S. C.; Kroutchinina, N.; Khandurina, J.; Foote, R. S.; Ramsey, J. M. *Anal. Chem.* **1998**, *70*, 158−162.

10.1021/ac035310p CCC: $27.50
Published on Web 04/27/2004

and included both static[6,7,9−16] and flow-through systems[17,18] as well as contact and noncontact heating.[15] Drawbacks to these methods include high template concentrations,[18] inability to integrate into a fluorescence detection system,[7,18] and for genetic analyses relatively large sample volumes.[9,10] More recent work in our group has yielded a monolithic integrated PCR-CE system with valves and vents for sample positioning and immobilization, small chamber volumes (200−280 nL), and cycling times of only 10 min.[19] The ultimate sensitivity of this device has been demonstrated by performing stochastic PCR to the single-template molecule limit.[20] Most recently, we have described a fully integrated laboratory-based device including microfabricated heaters and resistance temperature detectors (RTDs) within the PCR chambers.[21] These added components improve the overall thermal transfer from the heating element to the PCR chamber, increase heating and cooling rates, and increase the accuracy of the temperature measurement. The efficacy of this microsystem was demonstrated by performing a multiplex sex determination assay from human genomic DNA.[21] Most recently, Koh and co-workers[22] described a PCR-CE device for a clinical diagnostics application starting from intact *Escherichia coli* cells. Their PCR-CE microdevice, while fully integrated, required a laboratory bench-sized laser excitation and observation system as in previous work.

Work toward the development of portable real-time PCR systems has also progressed significantly. Belgrader et al.[23] presented a real-time homogeneous PCR system based on the original work by Northrup et al.[24] Higgins and co-workers recently demonstrated detection of pathogenic strains of *E. coli* using a portable real-time thermal cycler.[25] However, real-time PCR can suffer from sensitivity to nonspecific PCR amplification and limited multiplexing due to the spectral overlap of fluorescent dyes. Although melt analysis can be used as an indirect measure of product size, small differences between false amplicons and correct product sizes can be difficult to distinguish using this method. The PCR-CE devices mentioned above exploit the product size information afforded by CE separation to avoid such problems. Portable instruments that can perform rapid integrated nanoliter-volume PCR amplification with a product analysis step such as microchannel capillary electrophoresis have not been demonstrated and would greatly enhance the ability of public health officials and researchers to discover, diagnose, and prevent pathogenic disease.

Here we present the design and fabrication of a new PCR-CE microsystem and the development of a portable analysis instrument that contains all the necessary operational electronics and optics for clinical diagnostics and pathogen detection applications. To demonstrate the utility of this system for rapid analysis from complex sample mixtures, we perform two separate pathogen detection experiments. The first assay probes for the presence of pathogenic *E. coli* O157:H7, a major foodborne pathogen, which is estimated to cause 20 000 infections a year in the United States alone.[26] Our PCR-CE assay tests for the presence of three separate markers that differentiate between three different strains of *E. coli*: a laboratory strain K12, an "atypical" enteropathogenic *E. coli* EPEC strain O55:H7, and an enterohemorrhagic, shigatoxin-producing *E. coli* (EHEC/STEC) strain O157:H7. The second assay detects the presence of the methicillin-resistance gene in *Staphylococcus aureus.* Multiplex PCR is used to detect a marker specific to *S. aureus* as well as an antibiotic resistance marker.

To facilitate the development of this more complex and portable integrated PCR-CE system, it was necessary to combine our previous work on PCR-CE chips with novel PDMS valves on glass microdevices described recently by Grover et al.[27] Our previous PCR-CE devices utilized a microfluidic containment system composed of drilled valves and hydrophobic vents, containing manually placed active or passive membranes, a design modeled after that presented by Anderson et al.[28] This approach has notable advantages, including sensorless sample positioning and bubble evacuation. However, the latex microvalve technology has large 50-nL dead volumes per element and requires manual construction. The dead volumes for our PDMS valves can be as small as 8 nL, and three valves in series form versatile membrane diaphragm pumps. These valves are advantageous over both our previous designs and other PDMS valve designs[29] because they are normally closed, can be actuated with small pressures and vacuums, and minimize PDMS solution contact to avoid the well-known chemical absorption and fluorescence background problems of PDMS. The integrated microsystem presented here combines previous accomplishments with new PDMS valve isolation. This analysis instrument is the first such integrated device to be employed for the analysis of pathogenic organisms.

EXPERIMENTAL SECTION

Device Design Overview. The mask design used for fabrication of the PCR-CE device is presented in Figure 1A. The device consists of a single PCR-CE system fabricated in a glass wafer sandwich the size of a microscope slide. The 200-nL PCR chamber is connected to a loading port on each side through microfluidic PDMS valves. Each valve consists of a PDMS membrane sandwiched between a drilled external displacement chamber and two drilled fluidic ports (Figure 1B). One port on each valve connects to the loading reservoir, while the other ports connect to the

(11) Zhang, N. Y.; Yeung, E. S. *J. Chromatogr., B* **1998**, *714*, 3−11.
(12) Zhang, N. Y.; Tan, H. D.; Yeung, E. S. *Anal. Chem.* **1999**, *71*, 1138−1145.
(13) Poser, S.; Schulz, T.; Dillner, U.; Baier, V.; Kohler, J. M.; Schimkat, D.; Mayer, G.; Siebert, A. *Sens. Actuators, A* **1997**, *62*, 672−675.
(14) Northrup, M. A.; Ching, M. T.; White, R. M.; Watson, R. T. *DNA Amplification with a Microfabricated Reaction Chamber*; Institute of Electrical and Electronic Engineers: Yokahama, Japan, 1993; pp 924−926.
(15) Oda, R. P.; Strausbauch, M. A.; Huhmer, A. F. R.; Borson, N.; Jurrens, S. R.; Craighead, J.; Wettstein, P. J.; Eckloff, B.; Kline, B.; Landers, J. P. *Anal. Chem.* **1998**, *70*, 4361−4368.
(16) Ibrahim, M. S.; Lofts, R. S.; Jahrling, P. B.; Henchal, E. A.; Weedn, V. W.; Northrup, M. A.; Belgrader, P. *Anal. Chem.* **1998**, *70*, 2013−2017.
(17) Schneegass, I.; Brautigam, R.; Kohler, J. M. *Lab Chip* **2001**, *1*, 42−49.
(18) Kopp, M. U.; de Mello, A. J.; Manz, A. *Science* **1998**, *280*, 1046−1048.
(19) Lagally, E. T.; Simpson, P. C.; Mathies, R. A. *Sens. Actuators, B* **2000**, *63*, 138−146.
(20) Lagally, E. T.; Medintz, I.; Mathies, R. A. *Anal. Chem.* **2001**, *73*, 565−570.
(21) Lagally, E. T.; Emrich, C. A.; Mathies, R. A. *Lab Chip* **2001**, *1*, 102−107.
(22) Koh, C. G.; Tan, W.; Zhao, M. Q.; Ricco, A. J.; Fan, Z. H. *Anal. Chem.* **2003**, *75*, 4591−4598.
(23) Belgrader, P.; Young, S.; Yuan, B.; Primeau, M.; Christel, L. A.; Pourahmadi, F.; Northrup, M. A. *Anal. Chem.* **2001**, *73*, 286−289.
(24) Northrup, M. A.; Benett, B.; Hadley, D.; Landre, P.; Lehew, S.; Richards, J.; Stratton, P. *Anal. Chem.* **1998**, *70*, 918−922.
(25) Higgins, J. A.; Nasarabadi, S.; Karns, J. S.; Shelton, D. R.; Cooper, M.; Gbakima, A.; Koopman, R. P. *Biosens. Bioelectron.* **2003**, *18*, 1115−1123.
(26) Boyce, T. G.; Swerdlow, D. L.; Griffin, P. M. *N. Engl. J. Med.* **1995**, *333*, 364−368.
(27) Grover, W. H.; Skelley, A. M.; Liu, C. N.; Lagally, E. T.; Mathies, R. A. *Sens. Actuators, B* **2003**, *89*, 315−323.
(28) Anderson, R. C.; Su, X.; Bogdan, G. J.; Fenton, J. *Nucleic Acids Res.* **2000**, *28*, e60.
(29) Thorsen, T.; Maerkl, S. J.; Quake, S. R. *Science* **2002**, *298*, 580−584.

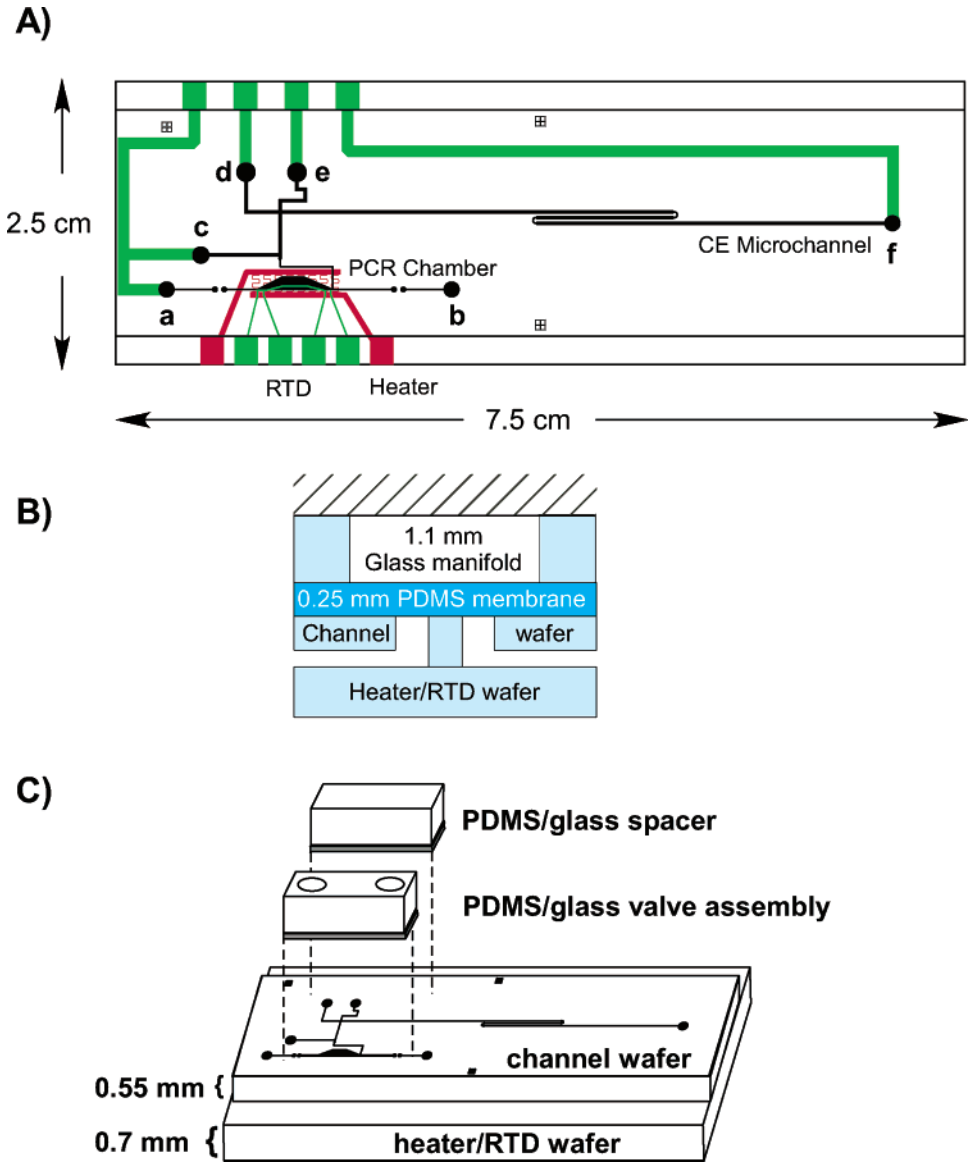

Figure 1. (A) Mask design for the portable PCR-CE microchip. The glass microchannels are indicated in black, the RTD and microfabricated electrodes are in green, and the heater (located on the backside of the device) is shown in red. The PCR chamber is loaded through reservoirs a and b. Reservoir c is the co-inject reservoir, d is the cathode, e is the waste, and f is the anode. (B) Schematic side view of a PDMS microvalve. (C) Exploded view of the assembly of the PCR-CE microchip, showing PDMS microvalve construction and PDMS gaskets.

chamber. The injection channel and PCR chamber geometries were optimized to facilitate loading the viscous linear polyacrylamide separation matrix. Cross-arms from the injection cross to the cathode and waste were made equal in length, and the injection channel to the PCR chamber was moved from the center of the chamber to one end to ensure that the matrix did not enter the main section of the PCR chamber. A co-injection channel is incorporated between the PCR chamber and the injection cross for introduction of a sizing ladder. Due to physical constraints, the position of the co-injection reservoir was fixed and thus the co-injection cross channel width was increased to balance gel loading. The separation system used for this study consists of a 7-cm-long CE channel with optimized low-dispersion hyperturns.[30] The PCR chamber and capillary electrophoresis channels are etched into one glass substrate, and a four-wire RTD and heater are fabricated on a second, flat glass substrate. The RTD is fabricated so that it lies inside the PCR chamber after thermal compression bonding of the two substrates. Optional microfabricated electrodes may also be patterned at the same time as the RTDs for application of the capillary electrophoresis voltages.

Microfabrication. The microfabrication process is nearly identical to that presented earlier.[21] Briefly, 550-μm D263 glass wafers were cleaned before sputter deposition of a 2000-Å layer of amorphous silicon. Photoresist was spun on and photolithographically patterned using a contact aligner, and the underlying silicon etch mask was selectively removed by reactive ion etching. Next, the fluidic channels, electrophoresis channels, and PCR chambers were etched to a depth of 36 μm. Reservoir access holes (1.5-mm diameter) and fluidic via holes (0.020-in. diameter) for the PDMS valves were drilled with diamond bits. The wafer was then diced to form two 20 mm $\times$ 75 mm slides.

(30) Paegel, B. M.; Hutt, L. D.; Simpson, P. C.; Mathies, R. A. *Anal. Chem.* **2000**, *72*, 3030−3037.

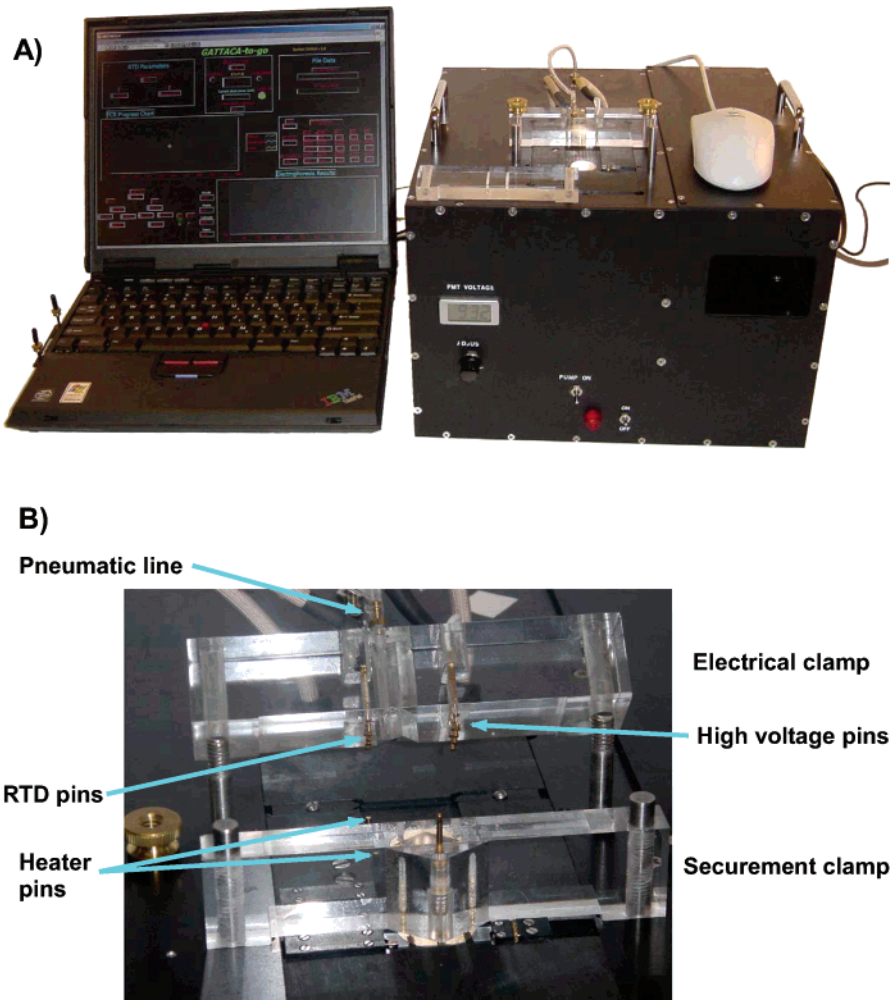

Figure 2. (A) Photograph of the portable PCR-CE analysis system. The analysis system box has dimensions 8 in. × 10 in. × 12 in., and the front panel has controls for power, PMT voltage, and pneumatic pump power. The clamps used to fix the microchip in place are shown on top of the analysis box. (B) Close-up of the two clamps used to fix the microchip in place during use. In foreground, the securement clamp; in the background, the electrical clamp with spring-loaded pins for RTD electrical connection and high-voltage electrodes. Design details and schematics will be found at http://www.cchem.berkeley.edu/ramgrp/portsup.

To form the RTDs and electrodes, a 550-μm-thick D263 wafer was first sputter-coated with 200 Å of Ti and 2000 Å of Pt. Thick photoresist was spun on and patterned. Following hard baking of the photoresist, the metal was etched using hot aqua regia (3:1 HCl/HNO_3, 90 °C) to form the RTD elements.

The integrated heaters were formed by first depositing a multilayer thin film of 200 Å of Ti and 2000 Å of Pt on the backside of the RTD wafer using rf sputtering. Thick photoresist was spun on this side; the wafer was patterned using a backside contact aligner and hard baked. Gold was electrodeposited onto the Ti/Pt seed layer to a 5-μm thickness to form the heater leads. The photoresist was removed, and the backside was repatterned using thick photoresist. The heating elements were etched into the Ti/Pt seed layer using an ion beam etching system. The RTD/heater wafer was diced into two 25 mm × 75 mm slides. The drilled channel wafer was thermally bonded to the RTD/heater wafer using a programmable vacuum furnace.

The valves were assembled after bonding in a manner similar to that outlined by Grover et al.[27] Briefly, a PDMS membrane (254-μm-thick HT-6240, Bisco Silicones, Elk Grove, IL) was applied to the bonded channel/RTD wafer stack. This assembly and a diced glass manifold and spacer were separately cleaned in a UV−ozone cleaner (Jelight Co. Inc., Irvine, CA) and then irreversibly bonded at room temperature for 2 h. The channel surfaces were coated using a modified version of the Hjertén coating protocol,[31] and the RTDs were calibrated as described previously.[21] Further microfabrication details can be found in ref 32.

Instrumentation. The complete instrument used to perform analyses with the microdevice is shown in Figure 2. The instrument contains a 488-nm frequency-doubled diode laser operating at power levels up to 20 mW, dichroic beam splitters and confocal fluorescence excitation, and photomultiplier detection. The beam from the laser (Protera, Novalux Corp., Sunnyvale, CA) is reflected by a dichroic mirror (505DCXT, Chroma Technology Corp., Brattleborro, VT) that passes wavelengths longer than 500 nm. The filtered beam is reflected by a dichroic beam splitter (510 DRLP, Chroma) and is focused into the microchannel with an objective (0.70-mm focal length in D263 glass) constructed using an aspheric (350140, Light Path Technologies, Orlando, FL) and

(31) Hjerten, S. *J. Chromatogr.* **1985**, *347*, 191−198.
(32) Simpson, P. C.; Woolley, A. T.; Mathies, R. A. *J. Biomed. Microdevices* **1998**, *1*, 7−26.

planoconvex lens (45224, Edmund Industrial Optics, Barrington, NJ) yielding a 0.88 NA in the object space. The laser spot diameter in the microchannel is ~20 μm. The returning fluorescence passes through the dichroic beam splitter, through a band-pass filter (E510LP, Chroma Technology), and is focused with an achromat lens (45206, Edmund Industrial Optics) onto a 400-μm pinhole that is mounted on the face of a photomultiplier (HC120-07, Hamamatsu Corp, Bridgewater, NJ). The dye-labeled DNA fragments were excited with a laser power of 2 mW focused 6 mm from the anode well. The analog voltages from the PMT were processed using an active 5-Hz low-pass filter and collected using a National Instruments DAQ board (PCI-MIO-16XE−50) at 10 Hz.

The microdevice is inserted into a recessed area on the top of the instrument and held in place with two separate plexiglass clamps, shown in Figure 2B. The clamp at the far end contains spring-loaded electrical contacts that connect to the sample, waste, cathode, and anode electrodes on the microdevice and similar contacts for powering and sensing the RTD. Power for the heater is supplied through two spring-loaded pins that protrude from the bottom of the recessed area and contact pads on the bottom of the microdevice. A spring-loaded pin and thumbwheel assembly are used at the edge of the chip for lateral alignment of the CE microchannel with the fixed position of the objective focus. The plexiglass clamping assembly at the near end has two spring-loaded pins that are used to hold the microdevice against the face of the objective.

The valves on both sides of the PCR chamber were opened and closed using vacuum or pressure supplied through a tube connected to the electrical clamp. Pressure and vacuum were supplied by a small rotary pump (G12/02-8-LC, Thomas, Sheboygan, WI) and two solenoid valves (H010E1, Humphrey, Kalamazoo, MI) inside the instrument. The clamp used in these experiments also contained Pt electrodes that protrude through the bottom of the plexiglass clamps and are positioned within the drilled reservoirs on the microchip for application of high voltage during CE; a separate wire is connected to the anode pin position in the securement clamp. Such electrodes are not necessary if the microfabricated electrodes are included in the design.

A custom-built precision current source was used to supply 4 mA to the RTD, and the voltage across the RTD was collected and filtered using an active low-pass filter operating at 5 Hz. Temperature control was accomplished through a proportion/integrator/differentiator module within a LabVIEW (National Instruments, Austin, TX) program. DAC output from the computer controls a current source circuit inside the instrument to supply the power necessary to drive the heaters. Further design details and schematics will be found at http://www.cchem.berkeley.edu/ramgrp/portsup.

The PCR-CE microdevices were filled with the linear polyacrylamide by forcing the solution through the entire microfluidic system from the anode using a syringe. The channel design prevented the gel from entering the PCR chamber, but the gel plug in the loading channel forms a passive barrier to the flow of reagents from the PCR chamber into the separation channel during amplification as first introduced by Woolley et al.[5] Buffer (1× TTE) was loaded into the waste, cathode, and anode reservoirs with a pipet after gel loading. The sample was introduced at reservoir a (Figure 1A) with a pipet. Vacuum applied at reservoir b (Figure 1A) moved the sample through the valve and into the PCR chamber. The valves were then closed to prevent sample movement during heating. Bubble-free loading was consistently achieved using this methodology.

Bacterial Culture and Dilution. *E. coli* K12 cells transformed with a TOPO plasmid (Invitrogen Technologies, Carlsbad, CA) conferring antibiotic resistance to ampicillin and kanamycin were grown overnight at 37 °C on LB agar plates. Colonies were picked and suspended in minimal LB broth with 25 μg/mL kanamycin and grown overnight at 37 °C. *E. coli* O157:H7 cells were streaked from agar slants onto EMB plates and grown overnight at 37 °C. Colonies were picked from the plates, suspended in LB media, and grown overnight at 37 °C. *E. coli* O55:H7 cells were streaked from agar slants onto blood agar plates and grown overnight at 37 °C. Colonies were picked from the plates, suspended in LB media, and grown overnight at 37 °C. Cell density was quantitated by optical density determination of the broth/cell suspension at 600 nm with a UV−visible spectrophotometer (Jasco, Easton, MD). The cells were washed three times in 1 mL of phosphate-buffered saline (pH 7.4). The cells were then suspended in sterile deionized water to an approximate concentration of 10 000 cells/μL and immediately added to the appropriate PCR mixtures.

Methicillin-resistant *S. aureus* (MRSA) and methicillin-sensitive *S. aureus* (MSSA) cells were grown overnight on blood agar plates (5% sheep blood, Hardy Diagnostics, Santa Maria, CA) at 30 °C. Colonies were picked, suspended in 10 mL of YPC media, and incubated at 30 °C overnight. Cells were quantitated by serial dilutions in YPC media plated onto blood agar plates. Colony-forming units were counted, and a dilution of the original liquid stock was made in sterile deionized water to form a working concentration of 10 000 cells/μL.

For the commensal *E. coli* dilution experiments, the cell concentrations were measured using a UV−visible spectrophotometer at 600 nm. This measurement was externally calibrated by performing a serial dilution of the original stock, plating a known volume of cells from each dilution onto LB agar plates, and counting the colonies after incubation at 37 °C overnight. A serial dilution from the original stock then gave the desired cell concentrations and mixtures. These cell suspensions were added to the PCR mixture as indicated previously and amplified using the same PCR protocol, except that only 30 cycles were used.

PCR Amplification and Capillary Electrophoresis. The CE separation medium was a nondenaturing 3.5% linear polyacrylamide matrix, prepared by dissolving acrylamide monomer in 25 mL of 1× TTE buffer and subsequently polymerizing overnight under argon at room temperature. The double-stranded DNA sizing ladder used in these experiments was custom-made using PCR amplification. In this construction, the forward primer for all amplicons was a 6-carboxyfluorescein (FAM)-labeled primer (Integrated DNA Technologies, Coralville, IA) complementary to the region upstream of the insertion site of the M13/pUC19 cloning vector (Invitrogen Technologies). The reverse primers were chosen to yield specific fragment lengths that would not overlap with the product sizes of the PCR products of interest. The bands were 111, 152, 195, 267, 319, and 414 bp. Following PCR amplification, the ladder was purified using a centrifugation column to remove residual primers and excess salt (Amersham

Table 1. PCR Primer Sequences and Product Lengths

assay	forward primer	reverse primer	product sizes
E. coli	species-specific 16S:[a] 5′-[6-FAM]-CGCTTACCACTTTGTGATT-3′	species-specific 16S: 5′-ATTAAGGCAGGTGACTTTCA-3′	species specific: 280 bp
	fliC:[b] 5′-CAGGTCTTTATGGTCTGAAA-3′	*fliC*: 5′-[6-FAM]-ATGGTGATATTACCTGCTGA-3′	*fliC*: 625 bp
	sltI:[c] 5′-[6-FAM]-CAGTTAATGTGGTGGCGAAGG-3′	*sltI*: 5′-CACCAGACAATGTAACCGCTH-3′	*sltI*: 348 bp
MRSA[d]	*femA*: 5′-[6-FAM]-CTTACTTACTGCTGTACCTG-3′	*femA*: 5′-ATGTCGCTTGTTATGTGC-3′	*femA*: 219 bp
	mecA: 5′-[6-FAM]-TGGCTATCGTGTCACAATCG-3′	*mecA*: 5′-CTGGAACTTGTTGAGCAGAG-3′	*mecA*: 310 bp

[a] Based on Greisen et al.[34] [b] Based on Gannon et al.[35] [c] From Cebula et al.[36] [d] Based on Vannuffel et al.[40]

Table 2. Thermal Cycling Conditions

assay	hotstart	denature	anneal	extend	no. of cycles
S. aureus	95 °C, 1 min	94 °C, 10 s	55 °C, 15 s	72 °C, 15 s	30
E. coli	95 °C, 1 min	94 °C, 10 s	step-down: 64 °C 5×, 62 °C 5×, 60 °C 25×	72 °C, 15 s	35

Biosciences, Piscataway, NJ) and different product lengths were pooled to yield the final ladders.

The PCR primers used to amplify each genetic marker are presented in Table 1, along with the expected product sizes. Primers were added to a final concentration of 200 nM in the *S. aureus* assay; primer concentrations in the *E. coli* assay were 200 nM for each of the *sltI* and *fliC* primers and 400 nM for the 16S primers. Other reaction components included 1× PCR buffer, 100 μM concentrations of each dNTP, 1.5 mM $MgCl_2$, 100 μg/mL bovine serum albumin, and 1.5 units of hot start *Taq* polymerase (Platinum Taq, Invitrogen Technologies). Multiplex reactions were optimized using a gradient thermal cycler (Eppendorf, Westbury, NY). The thermal cycling profiles for each assay are presented in Table 2. The *E. coli* assay utilized a step-down PCR method because the three primer sets had slightly different melting temperatures. Following microchip PCR amplification, the sample and DNA ladder were co-injected into the CE channel using a pinched injection with a field strength of 112 V/cm and then separated by applying a field strength of 165 V/cm while back-biasing the sample and waste reservoirs. The microdevice was cleaned after each analysis by flushing the channels and the PCR chamber with deionized water.

RESULTS AND DISCUSSION

***E. coli* Pathovar Detection.** Rapid and robust detection of infectious disease agents is an active area of current interest and research in public health and domestic security. Two representative bacterial pathogens, *E. coli* and *S. aureus*, are the major focus of this study. *E. coli* remains one of the most common causes of infectious diseases worldwide. It is responsible for a variety of diseases, including diarrhea, urinary tract infections, bacteremia, meningitis, and wound infections. However, *E. coli* is also a commensal bacterial organism ubiquitous in mammalian intestines as well as in the environment. Hence, the rapid differentiation of nonpathogenic, commensal *E. coli* from pathogenic variants (pathovars) is a major clinical and public health concern.

There are at least four major groups of *E. coli* known to cause diarrheal diseases in humans: ETEC (enterotoxigenic *E. coli*), EPEC (enteropathogenic *E. coli*), EIEC (enteroinvasive *E. coli*), and STEC (shigatoxin-producing *E. coli*)[33] which differ in their methods of pathogenesis. The differentiation of *E. coli* pathovars from commensal *E. coli* relies on the detection of gene sequences that encode pathovar-specific virulence factors such as the shigatoxin of STEC. The three primer sets used in our multiplex amplification included *E. coli* 16S rRNA species-specific primers (after ref 34), primers specific for a portion of the *fliC* gene encoding the *E. coli* H7 flagellar antigen,[35] and primers specific for the shigatoxin I *(sltI)* gene present in enterohemorrhagic strains of *E. coli* such as O157:H7.[36] *E. coli* O157:H7, which also belongs to the enterohemorrhagic *E. coli* (EHEC) group, is the most common STEC strain causing bloody diarrhea, associated with contaminated food in the United States. There are many other serotypes of STEC; thus, *E. coli* O157:H7 is further differentiated from other STEC strains by the detection of its H7 flagellar antigen gene as well as the *sltI* gene encoding shigatoxin I. *E. coli* O55:H7 is a member of the "atypical" EPEC group, which causes infantile diarrhea and does not express shigatoxins.

Figure 3 presents results from a series of amplifications conducted directly from intact *E. coli* cells; each analysis took 30 min to complete. Panel A presents an amplification from *E. coli* K12 cells; only the species-specific product is observed at 280 bp. Panel B presents an amplification from *E. coli* O55:H7 cells. Both the 280-bp species-specific and the 625 bp *fliC* product are present, identifying the cell as an H7 serotype, but not producing shigatoxin. Finally, panel C presents an amplification conducted from *E. coli* O157:H7 cells. The additional presence of the 348-bp *sltI* peak clearly demonstrates that this sample is a shigatoxin-producing H7-expressing strain.

Additionally, we were interested in determining the minimum number of cells required to successfully perform an assay on our

(33) Bopp, C. A.; Brenner, F. W.; Fields, P. I.; Wells, J. G.; Strockbine, N. A. In *Manual of Clinical Microbiology*, 8 ed.; Murray, P. R., Braron, E. J., Jorgensen, J. H., Pfaller, M. A., Yolken, R. H., Eds.; ASM Press: Washington, DC, 2003; pp 654−671.
(34) Greisen, K.; Loeffelholz, M.; Purohit, A.; Leong, D. *J. Clin. Microbiol.* **1994**, *32*, 335−351.
(35) Gannon, V. P. J.; Dsouza, S.; Graham, T.; King, R. K.; Rahn, K.; Read, S. *J. Clin. Microbiol.* **1997**, *35*, 656−662.
(36) Cebula, T. A.; Payne, W. L.; Feng, P. *J. Clin. Microbiol.* **1995**, *33*, 248−250.

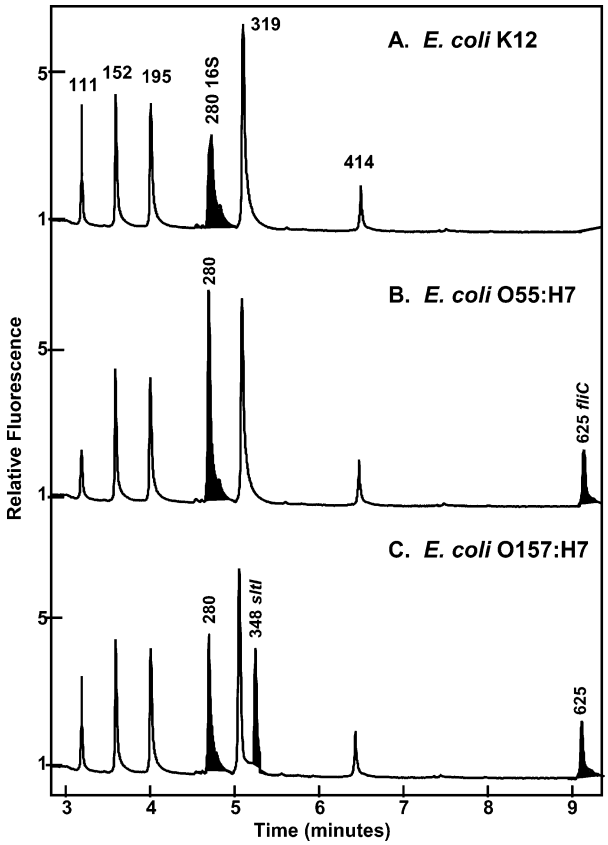

Figure 3. Pathogenic organism analysis conducted directly from intact *E. coli* cells using the portable PCR-CE microsystem. (A) Analysis conducted from *E. coli* K12 cells, showing only the presence of the co-injected DNA ladder and the 280-bp 16S species-specific amplicon. (B) Analysis conducted from *E. coli* O55:H7 cells, showing the ladder, the 280-bp 16S species-specific amplicon and the 625 bp *fliC* amplicon characteristic of cells presenting the H7 surface antigen. (C) Analysis conducted from *E. coli* O157:H7 cells, showing the DNA ladder, the 16S species-specific amplicon, the 625-bp *fliC* amplicon, and the 348-bp *sltI* amplicon, characteristic of *E. coli* both possessing an H7 antigen and expressing shigatoxin. Each analysis was conducted from a starting concentration of 40 cells in the reactor in a time of 30 min.

system and whether we could perform quantitation of bacterial cell concentration. To determine the molecular limits of detection, we conducted PCR-CE assays from varying concentrations of *E. coli* K12 cells. Peak areas were calculated, and the ratio of all peak areas was taken. Since the ratio of dye molecules to DNA product molecules is stoichiometric, peak areas correlate directly to PCR product concentration. Figure 4 presents a linear fit to the normalized 16S product peak area as a function of starting K12 concentration. Each data point consists of the average of three amplifications (30 cycles each), and all separations were performed in a single day. The fit has a high correlation constant ($R^2 = 0.991$), indicating that under the conditions used, the PCR amplification is a linear function of starting cell concentration and exhibits a 100-fold dynamic range. The fact that the fit extrapolates well to zero starting concentration demonstrates that amplification from a trace number of cells is feasible using our portable integrated system. The extrapolated molecular limit of detection is approximately 2−3 cells in the chamber. These data demonstrate that cells can be directly added to a PCR mixture and lysed, amplified, and detected on our device. This experiment further

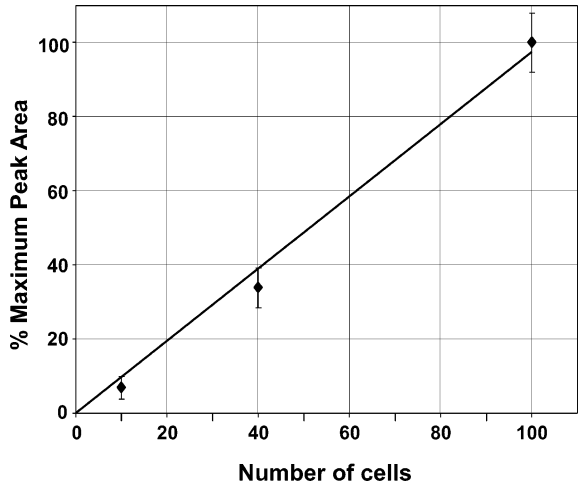

Figure 4. Plot of 16S product peak area as a function of calculated number of starting *E. coli* K12 cells in the chamber before amplification. For relatively small numbers of starting cells, reagent-limited saturation is not present, and the product peak area is a linear function of input DNA concentration ($R^2 = 0.991$). Error bars represent total observed range of peak area values. The limit of detection is 2−3 cells/reactor.

demonstrates the ability of our system to detect the serotype and pathogenic status of a given cell population simultaneously, a great benefit over standard approaches that detect only one or the other of these characteristics.[36] Now that the feasibility of this direct assay is demonstrated, we are exploring the use of different-sized reactors and the use of specific capture and concentration chambers to extend the dynamic range and concentration limit of detection.

***S. aureus* Analyses**. *S. aureus* is a Gram-positive pathogen that is responsible for a wide range of local and systemic infections. Antibiotic-resistant *S. aureus*, particularly methicillin-resistant strains, are a major problem in hospitals and are increasing in prevalence among community-acquired infections.[37] Facile differentiation of both species and antibiotic resistance information is therefore becoming increasingly important for treatment and prevention efforts. Methicillin resistance in *S. aureus* is encoded by the mecA gene carried by a DNA cassette inserted in the *S. aureus* chromosome. Two markers are commonly used in identifying methicillin resistance in *S. aureus* strains. The first marker, *mecA*, encodes PBP2, a penicillin-binding protein that provides β-lactam resistance.[38] The second marker, *femA*, is unique to *S. aureus* species and its detection serves to distinguish *S. aureus* from other staphylococcal species that carry methicillin resistance genes.[39] A *femA*/*mecA* multiplex amplification therefore provides species-specific identification simultaneously with methicillin resistance information.

Figure 5A presents a PCR-CE analysis conducted on our microdevice using intact MRSA cells. MRSA and MSSA *S. aureus* cells were introduced into separate PCR mixtures (final concentration 40 cells/reactor) and amplified in 18 min by a multiplex PCR with primers for the two markers. Note the presence of both

(37) Stevens, D. L. *Curr. Opin. Infect. Dis.* **2003**, *16*, 189−191.
(38) Hackbarth, C. J.; Chambers, H. F. *Antimicrob. Agents Chemother.* **1989**, *33*, 991−994.
(39) Bergerbachi, B.; Barberismaino, L.; Strassle, A.; Kayser, F. H. *Mol. Gen. Genet.* **1989**, *219*, 263−269.

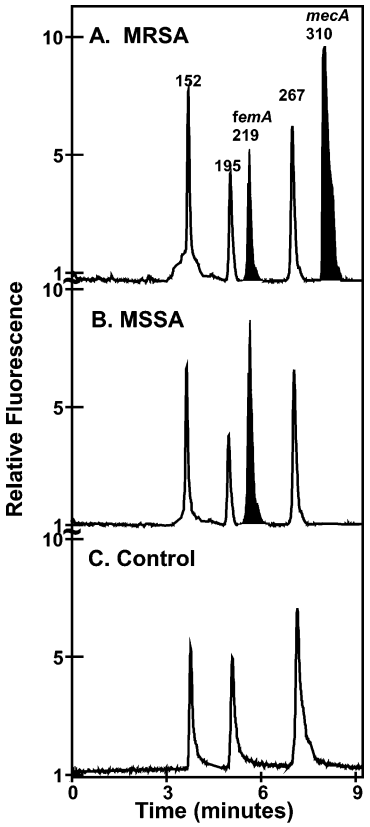

Figure 5. Pathogen analysis conducted directly from intact *S. aureus* cells, demonstrating antibiotic resistance detection using the portable PCR-CE microsystem. (A) Analysis conducted from MRSA cells, showing the DNA ladder, the 219-bp *femA* species-specific amplicon, and the 310-bp *mecA* methicillin resistance amplicon. (B) Analysis conducted from MSSA cells, showing the DNA ladder and only the *femA* species-specific amplicon. (C) Negative control amplified without cells present, showing only the presence of the co-injected DNA ladder. The total analysis time was 30 min for each sample.

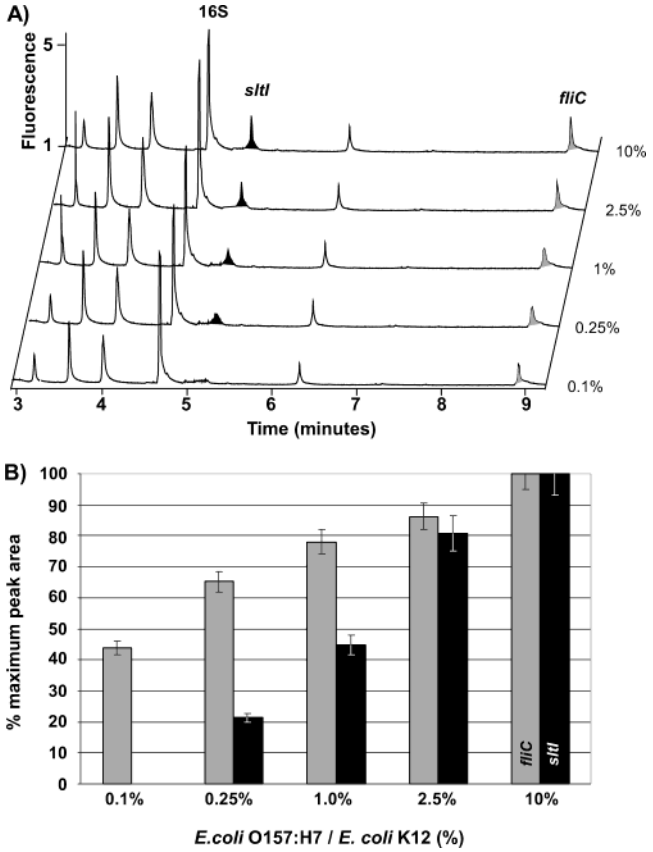

Figure 6. (A) Electropherograms generated from PCR-CE analyses of a serial dilution of *E. coli* O157:H7 cells in *E. coli* K12 cells. The relative percentages of *E. coli* O157:H7 in each analysis are presented on the right side. The total number of cells in each case was 10 000, and each analysis was performed with 30 PCR cycles. A decrease in both markers for pathovars (*sltI* and *fliC*) can be observed, with the *sltI* marker becoming limiting at 0.1%, or 1 cell in 1000. (B) A plot of the relative peak areas for both markers as a function of the dilution percentage.

peaks, *mecA* at 310 bp[40] and *femA* at 219 bp, in the MRSA analysis. The electropherogram in Figure 5B is generated after PCR amplification from MSSA cells and shows only the *femA* product peak, indicating the presence of methicillin-sensitive *S. aureus*. Figure 5C presents a negative control reaction run without cells, demonstrating that carryover contamination from previous reactions in the same chamber is not an issue at these cellular concentrations and conditions.

Detection with Commensal Background. The ability of an instrument and assay to detect pathovars in the presence of high commensal backgrounds is also critical, because this is the situation typically encountered with *E. coli* O157:H7 or other pathogenic *E. coli* infections. A serial dilution of *E. coli* O157:H7 cells into *E. coli* K12 cell concentrations generated a gradient of cell suspensions, with *E. coli* O157:H7 as the minor contributor. The percentage contribution of the O157:H7 serotype to each suspension was 10, 2.5, 1, 0.25, and 0.1% of the total number of cells. The total number of cells in these experiments was fixed at 10 000 in the PCR chamber before amplification, to ensure that, at the lowest O157:H7 concentrations, the number of these cells would remain outside the stochastic regime. Figure 6A presents a series of electropherograms generated after PCR amplification and separation from cell suspensions at each dilution point. These experiments utilized the microfabricated Pt electrodes on the microdevice. The limiting marker in these experiments was *sltI*, whose product disappeared only at the lowest dilution point, 0.1%. This demonstrates that our portable analysis instrument is capable of detecting as few as 10 *E. coli* O157:H7 cells in a background of 99 990 *E. coli* K12 cells, or 1 pathogenic cell in 1000 total *E. coli* cells. Figure 6B presents the relative decreases in measured product peak area for each of the two pathogenic markers at each dilution point. These data indicate that the system is capable of detecting pathogenic strains of *E. coli* at the lowest pathovar concentration presented here, since a *fliC* product is still present; however, since the *sltI* product is absent, a precise determination of the strain was not possible. Nevertheless, such a determination is probably useful, since even a preliminary finding of pathovars can indicate further testing in a clinical setting.

SUMMARY AND CONCLUSION

The genomic analysis system presented here is the first to combine microchip PCR amplification with capillary electrophoresis separation and detection in a fully integrated portable instrument. Analyses with this system are complete in less than 30 min,

(40) Vannuffel, P.; Laterre, P. F.; Bouyer, M.; Gigi, J.; Vandercam, B.; Reynaert, M.; Gala, J. L. *J. Clin. Microbiol.* **1998**, *36*, 2366−2368.

and we have demonstrated analyses of direct relevance to clinical diagnostics and pathogen detection. The reactor volume used here is small (200 nL), allowing sample and reagent conservation. The thermal cycling times (30 cycles in 20 min) are among the fastest ever demonstrated in a contact PCR-CE device. The current device also allows for multiplex reactions in a single PCR chamber; the number of possible simultaneous amplification products is determined by primer design, PCR reaction conditions, and our ability to electrophoretically distinguish the products. This allows for much more complicated multiplex assays to be conducted in this device and for assay flexibility as the pathogens are altered or mutate. The identification of the products produced by CE also provides verification of a successful background-free assay that will be critical for reducing false positives in high-throughput screening applications.

For future clinical diagnostic use it will be desirable to develop improved chip and instrument hardware as well as sample introduction methods and technologies to improve the limit-of-concentration detection. While the current glass chips can be effectively cleaned, the fabrication of inexpensive disposable chips would be valuable in a clinical setting.[41] We are currently working to further reduce the size of the analysis system, chiefly through reductions in the size of the laser and electronics modules inside the analysis instrument. Addition of microfabricated PDMS membrane pumps will facilitate automatic sample loading for a more robust analysis.[27] Finally, the current concentration limits of detection of 2−3 cells/200 nL are high (10 000/mL) and must be improved by integrated sample introduction. Now that we have a robust microanalyzer, we are working on adapting affinity capture methods[42,43] for sample preconcentration on these microdevices that will allow detection of trace concentrations of pathogens from large volumes and complex sample backgrounds.

(41) Andrisin, T. E.; Humma, L. M.; Johnson, J. A. *Pharmacotherapy* **2002**, *22*, 954−960.
(42) Paegel, B. M.; Yeung, S. H. I.; Mathies, R. A. *Anal. Chem.* **2002**, *74*, 5092−5098.
(43) Shelton, D. R.; Karns, J. S. *Appl. Environ. Microbiol.* **2001**, *67*, 2908−2915.

ACKNOWLEDGMENT

We thank the UC Berkeley Chemistry Machine Shop for construction of the portable analysis instrument and Henry Chan of the UC Berkeley Chemistry Electronics Shop for design and fabrication of the electronics. PCR-CE chip fabrication was performed at the University of California, Berkeley Microfabrication Laboratory. E.T.L. gratefully acknowledges the support of a Whitaker Predoctoral Fellowship. This research was supported by the NIH Grants AI056472, HG01399, and P01 CA77664.

Received for review November 6, 2003. Accepted March 14, 2004.

AC035310P